BIOLOGY OF REPRODUCTION **75,** 270–278 (2006)
Published online before print 10 May 2006.
DOI 10.1095/biolreprod.105.049684

Multiple Glycolytic Enzymes Are Tightly Bound to the Fibrous Sheath of Mouse Spermatozoa[1]

Michelle Krisfalusi,[3,4] Kiyoshi Miki,[3,5] Patricia L. Magyar,[3,4] and Deborah A. O'Brien[2,3,4,5]

Laboratories for Reproductive Biology,[3] Departments of Pediatrics[4] and Cell and Developmental Biology,[5] University of North Carolina School of Medicine, Chapel Hill, North Carolina 27599

ABSTRACT

The fibrous sheath is a cytoskeletal structure located in the principal piece of mammalian sperm flagella. Previous studies showed that glyceraldehyde 3-phosphate dehydrogenase, spermatogenic (GAPDHS), a germ cell-specific glycolytic isozyme that is required for sperm motility, is tightly bound to the fibrous sheath. To determine if other glycolytic enzymes are also bound to this cytoskeletal structure, we isolated highly purified fibrous sheath preparations from mouse epididymal sperm using a sequential extraction procedure. The isolated fibrous sheaths retain typical ultrastructural features and exhibit little contamination by axonemal or outer dense fiber proteins in Western blot analyses. Proteomic analysis using peptide-mass fingerprinting and MS/MS peptide fragment ion matching identified GAPDHS and two additional glycolytic enzyme subunits, the A isoform of aldolase 1 (ALDOA) and lactate dehydrogenase A (LDHA), in isolated fibrous sheaths. The presence of glycolytic enzymes in the fibrous sheath was also examined by Western blotting. In addition to GAPDHS, ALDOA, and LDHA, this method determined that pyruvate kinase is also tightly bound to the fibrous sheath. These data support a role for the fibrous sheath as a scaffold for anchoring multiple glycolytic enzymes along the length of the flagellum to provide a localized source of ATP that is essential for sperm motility.

fertilization, gamete biology, sperm, sperm motility and transport

INTRODUCTION

Spermatozoa are specialized both morphologically and biochemically to deliver the male genome to the egg. The sperm flagellum houses the machinery needed for motility and has a conserved structural organization among mammals. Like all flagella and cilia, the sperm tail has a centrally located axoneme that is essential for generating coordinated movement, a process that requires substantial amounts of ATP [1]. Structures surrounding the axoneme define distinct segments of the sperm flagellum, including the longest segment known as the principal piece. Mitochondria are confined to the middle piece of the sperm tail, presenting a challenge to the metabolic machinery to provide sufficient ATP to support motility along the entire length of the flagellum. It is now clear that several glycolytic enzymes are localized predominantly in the principal piece, including spermatogenic cell-specific hexokinase 1 variants (HK1S) [2, 3], glyceraldehyde-3-phosphate dehydrogenase, spermatogenic (GAPDHS) [4–6], enolase [7], and lactate dehydrogenase C (LDHC) [8]. This compartmentalization of glycolytic enzymes may be important for providing sufficient ATP to distal regions of the sperm flagellum [4, 5, 9–11]. Recent gene targeting studies indicate that GAPDHS is essential for sperm motility and male fertility and support the hypothesis that glycolysis generates most of the energy required for sperm motility [10].

Genetic analyses indicate that *Drosophila* cannot fly unless multiple glycolytic enzymes are specifically colocalized at the Z-discs and M-lines of the flight muscles [12, 13]. Similarly, we hypothesize that sperm motility depends on the colocalization of multiple glycolytic enzymes in the principal piece. GAPDHS, one of the novel glycolytic isozymes in sperm, is tightly bound to the fibrous sheath [4, 5], a cytoskeletal structure that defines the limits of the principal piece. The fibrous sheath lies just beneath the plasma membrane and consists of two longitudinal columns positioned 180° apart that are connected by closely arrayed transverse ribs [14]. Earlier studies found that many glycolytic enzymes in sperm are resistant to release by homogenization or hypotonic lysis, indicating that they may be bound to structural components of these cells [15, 16]. Subsequent studies in several mammalian species found that the fibrous sheath serves as a scaffold for a number of proteins, including metabolic enzymes and constituents of signaling pathways [reviewed in 17, 18]. Immunoelectron microscopy localized both GAPDHS [4, 19] and HK1S [2, 3] to the fibrous sheath. Only GAPDHS has been shown to remain associated with this cytoskeletal structure throughout rigorous extraction procedures [4, 5].

Although glycolysis is highly conserved, several sperm glycolytic enzymes have distinctive properties [20]. Like GAPDHS [21] and LDHC [22, 23], phosphoglycerate kinase 2 (PGK2) is encoded by a gene that is expressed only in spermatogenic cells [24, 25]. In addition, unique structural or functional properties have been reported for other glycolytic enzymes in spermatogenic cells and sperm, including HK1S [2, 3, 26], phosphoglucose isomerase [27], aldolase [28], triosephosphate isomerase [29], phosphoglycerate mutase [30], and enolase [7, 31]. Distinctive features of sperm glycolytic enzymes may be important for localization in the principal piece and/or altered regulation of this key metabolic pathway. To better understand the mechanisms responsible for the assembly and regulation of glycolysis in mammalian sperm, we used both proteomic and immunological approaches to determine if other glycolytic enzymes are tightly bound to the fibrous sheath. These studies are an essential step for determining how colocalization of glycolytic enzymes in the principal piece is achieved and if this structural organization is required for sperm motility.

[1]Supported by NICHD/NIH through U01 HD45982 and cooperative agreement U54 HD35041 as part of the Specialized Cooperative Centers Program in Reproductive Research and by the Andrew W. Mellon Foundation.
[2]Correspondence: Deborah A. O'Brien, Department of Cell and Developmental Biology, CB# 7090, University of North Carolina School of Medicine, Chapel Hill, NC 27599-7090.
FAX: 919 966 1856; e-mail: dao@med.unc.edu

Received: 28 November 2005.
First decision: 20 December 2005.
Accepted: 6 May 2006.

ISSN: 0006-3363. http://www.biolreprod.org

An important component of this study was to obtain fibrous sheath preparations with little contamination by other cytoskeletal structures, particularly the axoneme and outer dense fibers, which are associated with axonemal microtubule doublets in both the middle piece and the principal piece of the sperm flagellum. Olson and colleagues were the first to develop a sequential extraction procedure for isolating fibrous sheaths from rat sperm [32]. Similar procedures have been used to isolate fibrous sheaths from a number of mammalian species, including rat [33–36], mouse [19, 37], hamster [38], rabbit [39], humans [39, 40], and the brushtail possum [41]. In several of these studies [32–34, 41], electron micrographs detected filamentous material in the lumen of isolated fibrous sheaths, suggesting some contamination with other cytoskeletal remnants. Therefore, we modified the differential extraction procedure for fibrous sheath isolation and monitored purity with both electron microscopy and Western blotting. Using this procedure, we determined that enzymes in the sperm glycolytic pathway exhibit different solubilities and that several of these enzymes, in addition to GAPDHS, are tightly bound to the fibrous sheath.

MATERIALS AND METHODS

Animals and Sperm Collection

Adult CD-1 male mice were obtained from Charles River (Raleigh, NC). All investigations were approved by the University of North Carolina at Chapel Hill Animal Care and Use Committee and conducted in accordance with the Guide for the Care and Use of Laboratory Animals (Institute for Laboratory Animal Research, National Academy of Sciences).

For the collection of cauda epididymal sperm, epididymides were dissected from animals and immediately placed into cold PBS containing protease inhibitors (PBS + PI; 140 mM NaCl, 10 mM phosphate buffer, pH 7.4, Complete protease inhibitor cocktail [Roche Diagnostics, Mannheim, Germany]). Cauda were snipped multiple times, gently squeezed to liberate as many sperm as possible, and incubated at 37°C for 15 min to maximize sperm release. The sperm suspension was centrifuged at $1200 \times g$ for 5 min at 4°C and washed once with PBS + PI. After resuspending the pellet in PBS+ PI, the sperm were counted with a hemocytometer. Sperm counts throughout the enrichment procedure are referred to as sperm equivalents, as it was possible to generate an accurate sperm count only prior to sonication and/or extraction. Therefore, sperm equivalents (SE) throughout the extraction procedure are based on this initial count.

Fibrous Sheath Isolation

For each fibrous sheath isolation, $3–6 \times 10^8$ sperm were suspended in PBS + PI at a concentration of 8×10^7/ml. All steps in the procedure were done at 4°C. To separate sperm heads and tails and to break the flagella into pieces to allow for optimal penetration of extraction buffers, sperm were sonicated on ice with a prechilled probe for six 5-sec intervals at 40% output using a Branson Sonifier Cell Disruptor 185 (Danbury, CT). The sonicated sperm suspension was centrifuged at $2000 \times g$ for 5 min to pellet sperm heads, and the supernatant was removed and saved. The pellet was suspended in 12 ml PBS + PI, vortexed to release as many tails trapped within the pellet as possible, and centrifuged at $2000 \times g$ for 5 min. This was done three times, and each time the supernatant was collected. Supernatants were combined and centrifuged at $32\,500 \times g$ for 12 min to pellet tails. The tail pellet was frozen at −80°C until use. In some experiments the supernatant from the $32\,500 \times g$ centrifugation was precipitated with 10% (v/v) trichloracetic acid (TCA) to estimate the proportion of glycolytic enzymes released during the sonication and washing steps. Briefly, samples were vortexed after the addition of TCA, incubated on ice for 30 min, and centrifuged at $32\,500 \times g$ for 45 min. The pellets were washed with 100% ethanol and solubilized with SDS sample buffer. Densitometric scans of Western blots were used to estimate proportions solubilized by sonication.

Fibrous sheaths were isolated from sperm flagella according to the procedure developed by Olson and colleagues [32] with modifications. All extractions were carried out at 4°C with a concentration of 8×10^7 sperm equivalents/ml. The tail pellet was first extracted for 1 h with rocking in Triton X-100 extraction buffer (1% Triton X-100, 2 mM dithiothreitol [DTT], 1 mM EDTA, 1 mM EGTA, 2 mM PMSF, 50 mM Tris-HCl, pH 9.0, and Complete protease inhibitor cocktail [Roche]). The Triton-extracted sperm tails were pelleted by centrifugation at $32\,500 \times g$ for 12 min in a Sorvall RC 5C Plus centrifuge equipped with a fixed-angle SA-600 rotor. The pellet was resuspended in KSCN extraction buffer (0.6 M potassium thiocyanate [KSCN], 2 mM DTT, 50 mM Tris-HCl, pH 8.0) for 2 h with rocking, followed by centrifugation at $32\,500 \times g$ for 12 min. Final extraction of the pellet was carried out for 1 h with rocking in urea extraction buffer (6 M urea, 20 mM DTT, 50 mM Tris-HCl, pH 8.0). The pellet became more difficult to resuspend after each extraction step. It was critical to disrupt the pellet by vortexing and vigorous agitation prior to the addition of subsequent extraction buffers. Each extraction buffer was initially added dropwise with constant agitation until the pellet was dissolved. Failure to resuspend the pellets with this method resulted in inefficient extractions. The final fibrous sheath fraction was pelleted by centrifugation at $32\,500 \times g$ for 12 min. The pellets were either frozen at −80°C for later use, solubilized with SDS sample buffer for gel electrophoresis, or prepared for electron microscopy.

Following each extraction step, an aliquot was removed and centrifuged at $21\,000 \times g$ in a microcentrifuge for 10 min, and the pellet was solubilized in SDS sample buffer. Additionally, the supernatants were retained from each extraction and precipitated with 10% (v/v) TCA as described for the initial supernatant collected following sonication and centrifugation of the tail pellet. These samples were used to monitor the presence/absence of various flagellar proteins throughout the extraction procedure.

SDS-PAGE

SDS-PAGE was used to examine the proteins present at each step of the sperm fractionation procedure including the sperm tail fraction and both soluble and insoluble proteins remaining after treatment with the Triton X-100, KSCN, and urea extraction buffers. Proteins were heated for 5 min at 95°C in 2× SDS sample buffer (4% SDS, 100 mM DTT, 18 % glycerol, 125 mM Tris-HCl, pH 6.8) and separated on precast 10% polyacrylamide Tris-HCl Ready Gels (Bio-Rad, Hercules, CA). Following electrophoresis, the gel was fixed in 25% isopropanol and 10% acetic acid in deionized water for 1 h at room temperature with shaking. After removing the fixative, the gel was stained with SYPRO Ruby (Molecular Probes, Eugene, OR) overnight with shaking at room temperature. The gel was then rinsed for ~3 h with deionized water and transferred to 5% acetic acid. Protein bands were visualized and photographed with ultraviolet light. Samples were analyzed both on gels loaded with equal sperm equivalents and on gels with equal protein loads. Initial preparative gels were loaded with equal sperm equivalents and stained with SYPRO Ruby. After analyzing these gels by densitometry, protein loads were normalized to ensure equal protein loading on subsequent gels. BenchMark Protein Ladder (Invitrogen, Carlsbad, CA) was used to estimate the molecular weights of the proteins.

Western Blot Analysis

Proteins were electrophoretically transferred from gels to Immobilon-P transfer membrane (Millipore Corp., Bedford, MA) using the Ready Gel mini-gel tank transfer system (Bio-Rad). Membranes were stained with Coomassie G-250 staining solution (Bio-Rad) to verify the efficiency of the protein transfer. Blots were destained, rinsed with TBST (140 mM NaCl, 3 mM KCl, 0.05% Tween-20, 25 mM Tris-HCl, pH 7.4), and blocked with 5% skim milk in TBST for 30 min with shaking at room temperature. Blots were rinsed with TBST and incubated with primary antibody diluted in PBS containing 0.1% NaN_3 and 1% normal serum (goat or rabbit, matching the source of the secondary antibody) for 1 h at room temperature with rotation. After three 15-min washes with TBST, each membrane was incubated for 20 min at room temperature with the appropriate secondary antibody diluted in TBST. The blots were again washed three times with TBST (15 min each), and proteins were visualized by enhanced chemiluminescence using the SuperSignal West Pico substrate (Pierce, Rockford, IL).

Primary antibodies used for Western analysis included three rabbit antisera (gifts of Dr. E.M. Eddy, National Institute of Environmental Health Sciences) raised against peptides from the sequences of mouse A kinase (PRKA) anchor protein 4 (AKAP4, C-terminal peptide, 1:7500 dilution) [42], mouse HK1S (SSR peptide, 1:500 dilution) [2], and mouse GAPDHS (A1 peptide, 1:5000 dilution) [5]; rabbit antiserum against mouse PGK2 (1:1000 dilution, gift of Drs. John VandeBerg, Southwest Foundation for Biomedical Research, and John McCarrey, University of Texas at San Antonio); rabbit antiserum against rat outer dense fiber of sperm tails 2 (ODF2, 1:5000 dilution, gift of Dr. Frans van der Hoorn, University of Calgary) [43]; rabbit IgG against the mouse LDHC (1:1000 dilution, gift of Dr. Erwin Goldberg, Northwestern University) [44]; goat antiserum against rabbit muscle aldolase (1:5000, Rockland, Gilbertsville, PA); goat IgGs against rabbit muscle pyruvate kinase (1:1000 dilution, Polysciences, Warrington, PA), rabbit muscle LDH (1:500 dilution,

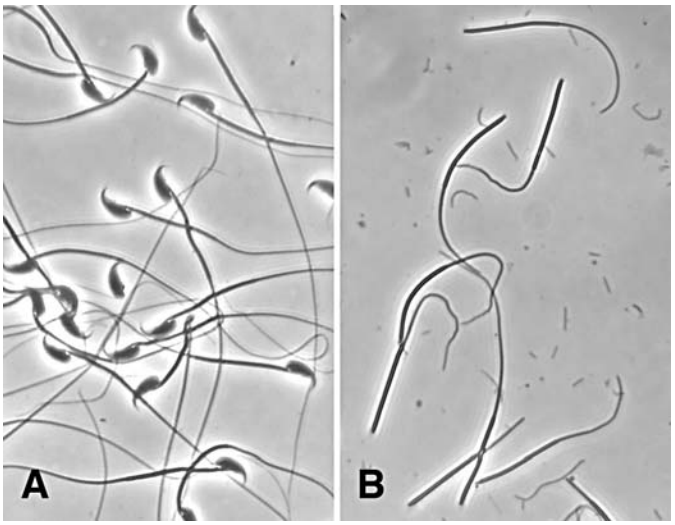

FIG. 1. Initial isolation of sperm flagella. Phase-contrast images are shown for intact mouse sperm (**A**) and fragmented flagella following brief sonication and removal of sperm heads by centrifugation (**B**). Original magnification ×500.

US Biologicals, Swampscott, MA), and human enolase (C-terminal peptide, 1:250 dilution, Santa Cruz, CA); and a mouse monoclonal IgG1 raised against chick brain tubulin (1:10 000 dilution, Sigma-Aldrich, St. Louis, MO). Affinity-purified horseradish peroxidase-conjugated secondary antibodies (KPL, Gaithersberg, MD) included goat anti-rabbit IgG (1:30 000 dilution), goat anti-mouse IgG (1:20 000 dilution), and rabbit anti-goat IgG (1:30 000 dilution).

Mass Spectrometry

For protein identification, fibrous sheath proteins isolated from 1.5×10^8 sperm were separated by SDS-PAGE using precast 10% polyacrylamide Tris-HCl gels and prepared for mass spectrometry (MS). The gels were fixed, stained with SYPRO Ruby (Molecular Probes), and transferred to 5% acetic acid as described previously. MS analysis was completed at the Michael Hooker Proteomics Core Facility at the University of North Carolina at Chapel Hill.

Peptide mass fingerprinting was carried out using a method previously described [45, 46]. SYPRO Ruby-stained gel bands were excised and digested overnight with trypsin using a ProGest digestor (Genomic Solutions, Ann Arbor, MI). The peptide extract was lyophilized overnight and resuspended in 20 μl of 50:50 methanol:water (0.1% formic acid) immediately prior to spotting. A saturated solution of recrystallized α-cyano 4-hydroxycinnamic acid (Sigma-Aldrich) in 50:50 acetonitrile:40 mM ammonium citrate in water (0.1% trifluoroacetic acid) was used as the matrix. A 0.3-μl aliquot of each sample was spotted and analyzed on an ABI 4700 TOF/TOF mass spectrometer, using the MALDI matrix. The peptide mass fingerprinting and sequence tag data from the TOF/TOF was searched using ABI's GPS Explorer scores, which are derived from Mascot searches (http://www.matrixscience.com).

For gel bands not identified using the previously mentioned protocol, a 6-μl aliquot of the extract was injected onto a Waters/Micromass API US Q-TOF mass spectrometer for liquid chromatography/MS/MS (LC/MS/MS) analysis. The LC/MS/MS instrument was equipped with an online Waters CapLC HPLC system. The Waters CapLC was outfitted with a Dionex C_{18} P3 trapping column (5 mm × 0.8 mm inner diameter [i.d.]) and a PepMap C_{18} capillary column (15 cm × 0.75 μm i.d.; Dionex, Sunnyvale, CA). A 75-min gradient from 5% CH_3CN to 80% CH_3CN (0.1% FA) was used. The mass spectra were scanned at 1 sec/scan over the mass range 400 to 1900 Da. MS/MS data were acquired over the mass range 50 to 1900 Da. Spectra were acquired in the "survey" mode, where an MS survey scan is acquired first, followed by MS/MS scans on parent ions meeting a preselected intensity threshold. For these experiments, the intensity threshold was set to "1" (the minimum allowable). The resulting MS/MS data were searched using the Mascot software package.

Electron Microscopy

Fibrous sheaths were isolated for whole-mount transmission electron microscopy and frozen in a 50% glycerol solution at −80°C. Whole mounts were prepared by glow discharging Pioloform-filmed nickel grids to render the surface hydrophilic, followed by floating the grids filmed side down on a droplet of fibrous sheath suspension for 5 min. Grids were rinsed briefly by floating on two drops of deionized water. The samples were negatively stained by floating on a drop of 2% aqueous uranyl acetate for 1 min. Grids were blotted with filter paper, allowed to air dry, and directly examined using a LEO EM-910 transmission electron microscope (LEO Electron Microscopy, Inc., Thornwood, NY) with an acceleration voltage of 80 kV. These studies were conducted in the Microscopy Services Laboratory in the Department of Laboratory Medicine and Pathology, University of North Carolina at Chapel Hill.

RESULTS

Fibrous Sheath Isolation

Approximately 95% of cauda sperm were decapitated by sonication for six 5-sec bursts at 40% output, and the sperm tails were fragmented into various-sized segments. The initial $2000 \times g$ centrifugation removed intact sperm and most of the sperm heads, along with some tail fragments. Phase-contrast microscopy indicated that the remaining sperm tail fraction contained a highly enriched fraction of flagella with <5% sperm heads (Fig. 1).

Following extraction of the sonicated sperm tails with buffers containing Triton X-100, KSCN, and urea, the fibrous sheath fraction was pelleted and examined by whole-mount electron microscopy (Fig. 2). This sequential extraction procedure solubilized most flagellar structures, including the plasma membrane, mitochondrial sheath, outer dense fibers, and axoneme. The remaining fibrous sheath fraction retained its typical ultrastructure, including both the longitudinal columns and the transverse ribs (Fig. 2, A–C). Cross-sectional views showed that the lumen of the fibrous sheath was generally free of debris and other cytoskeletal elements (Fig. 2C). The lumen of approximately 5%–10% of the longest fibrous sheath segments contained some filamentous material, likely to be microtubule or outer dense fiber remnants that resisted solubilization (arrow, Fig. 2D).

AKAP4 is the major fibrous sheath protein. It is present in both the longitudinal columns and the transverse ribs [47–49], is associated with multiple fibrous sheath constituents, and is important for assembly of the fibrous sheath [50–52]. Antibodies specific for AKAP4, an axonemal protein (α-tubulin), and an outer dense fiber protein (ODF2) were used for Western blot analysis to assess the elimination or retention of these cytoskeletal components throughout the extraction procedure (Fig. 3). AKAP4 was retained in the insoluble pellet fractions after each extraction, with only very small amounts of this fibrous sheath protein detected in the soluble supernatant fractions. These data support the electron microscopic evidence that the fibrous sheath remains intact. Both α-tubulin and ODF2 were prominent in the supernatant fractions but barely detectable in the fibrous sheath fraction that is pelleted after extraction with urea. These results confirm the purity of our fibrous sheath fraction and the effectiveness of our extraction procedure for the removal of axonemal and outer dense fiber constituents.

Polypeptide Composition of the Fibrous Sheath

Proteins in the fibrous sheath were separated by one-dimensional SDS-PAGE and identified by MS. A representative SYPRO Ruby-stained gel, with at least 18 distinct bands, is shown in Figure 4. Apparent molecular weights of bands 5–18 were estimated to be 110 000, 82 000, 67 000, 57 000, 56 000, 52 000, 50 000, 41 000, 37 000, 33 000, 32 000, 30 000, 28 000, and 27 000, while bands 1–4 appeared to be greater

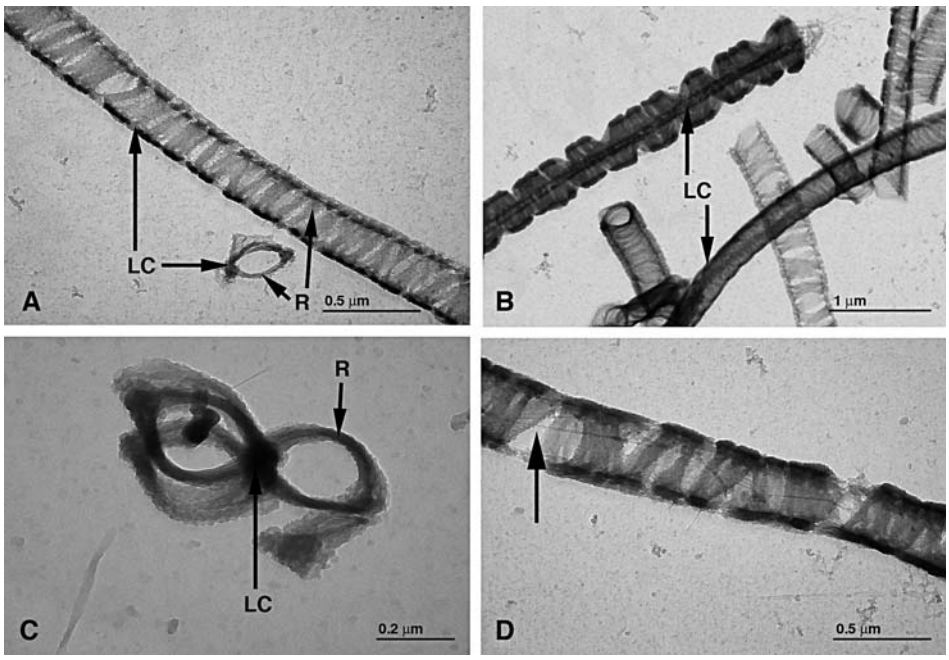

FIG. 2. Whole-mount electron microscopy of isolated fibrous sheaths. **A**) Longitudinal and cross-sectional views showing that the longitudinal columns (LC) and ribs (R) of the fibrous sheath are intact. **B**) Multiple longitudinal views showing different orientations of the fibrous sheath. **C**) Cross-sectional view showing that central flagellar structures, including the axoneme and outer dense fibers, are solubilized during the fibrous sheath extraction procedure. **D**) Longitudinal view showing filamentous material (arrow) within the lumen of a long fibrous sheath segment. Bar = 0.5 μm (**A**, **D**), 1 μm (**B**), 0.2 μm (**C**).

than 220 000. Six proteins were identified in 15 of the bands that were extracted and analyzed by peptide mass fingerprinting and MS/MS peptide fragment ion matching. The most abundant fibrous sheath constituent (band 6) was identified as AKAP4. The 110 000 molecular weight protein was identified as A kinase (PRKA) anchor protein 3 (AKAP3), the 67 000 band as GAPDHS, and the 27 000 band as glutathione S-transferase, mu 5 (GSTM5). The 50 000 and 41 000 molecular weight proteins were identified as aldolase 1, A isoform (ALDOA), and the 37 000 protein as lactate dehydrogenase A (LDHA). These seven protein bands were positively identified in at least two fibrous sheath samples, each with 3–24 peptides matching the theoretical digest of the identified protein. Additional proteins were not identified in these bands. Several minor bands (1–4, 8–10, and 14) were also identified as AKAP4, based on LC/MS/MS methods combined with

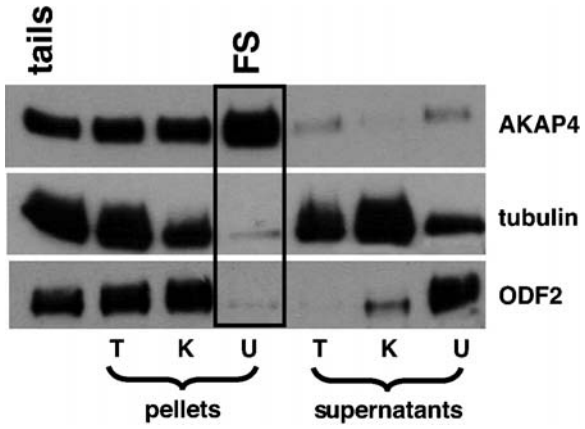

FIG. 3. Western blot analyses with antibodies to AKAP4, α-tubulin, and ODF2 to examine extraction of flagellar cytoskeletal components during the fibrous sheath isolation procedure. The first lane of each blot contains protein from flagella isolated from 10^6 sperm (tails). The tail fraction was sequentially extracted with buffers containing 1% Triton X-100 (T), 0.6 M KSCN (K), and 6 M urea (U), and aliquots were removed from each pellet and supernatant for Western analysis. The gels were loaded so that all lanes contain equal protein amounts. Isolated fibrous sheaths (FS) remain in the final urea pellet.

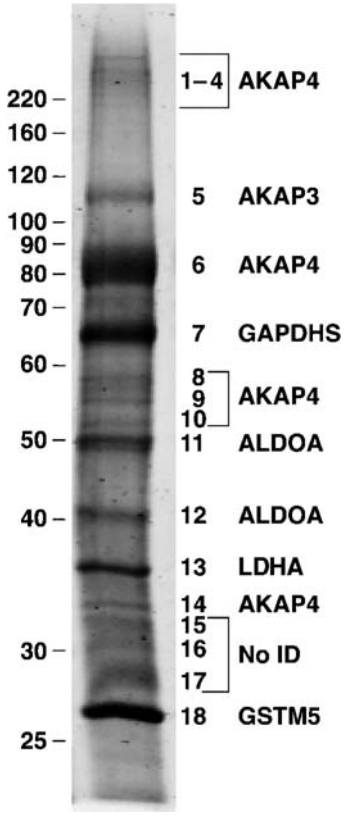

FIG. 4. Fibrous sheath protein identification. Proteins from the fibrous sheath fraction (1.5×10^8 sperm) were separated by SDS-PAGE. The gel was stained with SYPRO Ruby and samples from 18 bands were excised for proteomic analysis. Protein identifications determined by peptide-mass fingerprinting and MS/MS peptide fragment ion matching are indicated on the right. Relative molecular weights ($\times 10^3$) determined from standards are shown on the left.

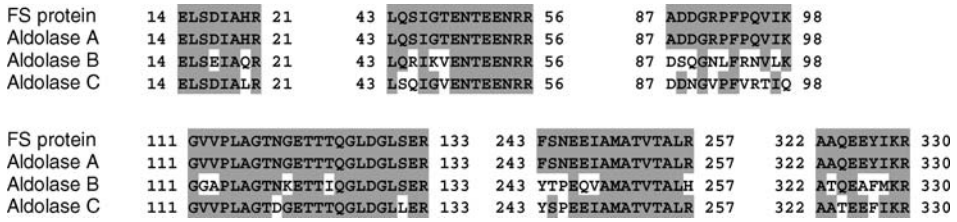

FIG. 5. Confirmation of ALDOA sequences in the fibrous sheath. Sequences in fibrous sheath (FS) proteins identified as ALDOA (bands 11 and 12 in Fig. 4) by MS/MS peptide fragment ion matching are compared to corresponding peptide sequences in mouse ALDOA, ALDOB, and ALDOC. The shaded areas indicate amino acid identities.

standard peptide mass fingerprinting and peptide fragment ion matching. The AKAP4 bands comprised approximately 50% of the total protein as determined by densitometry. The 28 000, 30 000 and 32 000 proteins (bands 15–17) failed to generate a positive identification. Proteins smaller than 20 000 were not detected in our analysis. In addition to AKAP4 [47, 48], previous studies have shown that AKAP3 [53], GAPDHS [4, 5], and GSTM5 [54] are associated with the fibrous sheath. ALDOA and LDHA, both components of tetrameric glycolytic enzymes, are newly identified constituents of the fibrous sheath fraction.

Confirmation of ALDOA and LDHA as Fibrous Sheath Constituents

Active aldolase and LDH enzymes are tetramers, each composed of one or more distinct subunit types. The three aldolase subunits and the three LDH subunits are each encoded by distinct genes, although there is significant sequence identity in each gene family. Therefore, we compared fibrous sheath sequences identified by MS/MS peptide fragment ion matching with all subunits in each family. Sequences identified in bands 11 and 12 were compared to mouse ALDOA (GenBank accession no. P05064), aldolase 2, B isoform (ALDOB, accession no. NP_659152), and aldolase 3, C isoform (ALDOC, accession no. P05063). Six peptide sequences showed 100% identity (81/81 amino acids) with ALDOA, whereas the percent identity with ALDOB and ALDOC were 64% (52/81 amino acids) and 79% (64/81 amino acids), respectively (Fig. 5). Similarly, the MS/MS peptide fragment ion sequences of band 13 were compared to the mouse LDHA (accession no. P06151), LDHB (accession no. P16125), and LDHC (accession no. P00342). These peptide sequences exhibited 100% identity (27/27 amino acids) with the LDHA subunit, compared to 56% identity (15/27 amino acids) with LDHB and 67% identity (18/27 amino acids) with LDHC (Fig. 6). These results confirm that both ALDOA and LDHA are present in the fibrous sheath.

Glycolytic Enzymes in the Fibrous Sheath

Multiple antibodies were used for Western blotting analysis to determine if other glycolytic enzymes are associated with the fibrous sheath. Four of the antibodies were specific for the spermatogenic cell-specific isozymes HK1S, GAPDHS, PGK2, and LDHC. Figure 7 shows the distribution of eight enzymes, arranged in descending order relative to the glycolytic pathway, throughout the fibrous sheath extraction procedure. All eight of these enzymes were present in the isolated sperm tail fraction (tails, first lane), although ~10%–20% of five glycolytic enzymes (H1KS, the larger ALDOA isoform, GAPDHS, pyruvate kinase, and LDHA) were lost during the initial sonication and washing steps. The proportions released by sonication were higher (~50%–70%) for PGK2, enolase, and LDHC. HK1S in the tail fraction was completely solubilized with Triton X-100 (T supernatant) and was not detected in subsequent fractions. Both ALDOA and GAPDHS were prominent constituents of the fibrous sheath fraction, although portions of these two enzymes were lost in the supernatant fractions. Two ALDOA bands were present in the fibrous sheath, with the same apparent molecular weights (50 000 and 41 000) as the bands identified as ALDOA by MS (bands 11 and 12 in Fig. 4). The smaller band exhibited less immunoreactivity with this aldolase antibody and more variability between preparations in the proportion released by sonication. A weak PGK2 band, approximately 5%–10% of that observed in the control tail sample, was sometimes detected in the fibrous sheath. The majority of the PGK2 in the tail fraction was solubilized with Triton X-100 and KSCN extraction buffers (T and K supernatants). Enolase was extracted with the KSCN buffer (K supernatant) and was not detected in the fibrous sheath fraction. Pyruvate kinase was retained in the fibrous sheath, with little immunoreactive protein present in the supernatant fractions. The testis-specific LDHC subunit was not detected in the fibrous sheath and was solubilized primarily with the KSCN extraction buffer (K supernatant). In contrast, LDHA was enriched in the fibrous sheath fraction. These results indicated that several glycolytic enzymes, in addition to GAPDHS [4, 5], are tightly associated with the fibrous sheath, particularly ALDOA, pyruvate kinase, and LDHA.

DISCUSSION

Both mouse and human sperm require glycolysis for motility and fertilization [10, 55, 56]. GAPDHS, one of the glycolytic isozymes that is specifically expressed in the male germ line, has been localized to the fibrous sheath in several mammalian species [4–6, 19] and has a novel proline-rich sequence at the N-terminus [21] that may mediate protein-protein interactions. This study demonstrates that the fibrous sheath acts as a scaffold for multiple glycolytic enzymes. In several somatic cell types, glycolytic enzymes associate with cytoskeletal and membrane proteins [57] and are sometimes enriched in subcellular compartments, including synaptic vesicles [58], postsynaptic densities [59], and specific regions

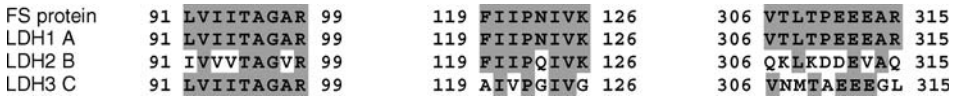

FIG. 6. Confirmation of LDHA sequences in the fibrous sheath. Sequences in the fibrous sheath (FS) protein identified as LDHA (band 13 in Fig. 4) by MS/MS peptide fragment ion matching are compared to corresponding peptide sequences of mouse LDHA, LDHB, and LDHC. The shaded areas indicate the amino acid identities.

within sarcomeres [12, 13]. Studies of *Drosophila* flight muscles are particularly striking because they demonstrate an essential structure-function relationship between the localization of glycolytic enzymes at Z-discs and M-lines and the ability to fly [12, 13, 57]. Similarly, the localization of sperm glycolytic enzymes to the fibrous sheath may be required for sperm function, providing a mechanism for localized ATP production in close proximity to the dynein ATPases that are distributed along the axoneme.

To begin testing this hypothesis and identifying protein interactions that are responsible for localization, we isolated fibrous sheaths and determined which glycolytic enzymes were tightly bound to this structure. The fibrous sheath isolation procedure used in this investigation was adapted from a technique developed by Olson and colleagues [32] to isolate the fibrous sheath from rat sperm. We found that the Olson procedure was quite effective and provided a very solid starting point for this study. However, our initial experiments with mouse sperm produced fibrous sheath fractions that were contaminated with other cytoskeletal proteins as monitored by Western blotting with antibodies to tubulin and outer dense fiber constituents. Modifications that improved the purity of our fibrous sheath fractions were controlled sonication to decapitate sperm and produce tail fragments, elimination of sperm nuclei early in the fractionation procedure, and reduction of the centrifugal force used to pellet the fibrous sheath following extraction with urea.

Although sonication has been used to isolate rat [33] and brushtail possum [41] sperm tails, shorter sonication bursts at reduced output were needed for the initial separation of mouse sperm heads and tails. Of critical importance to the success of this step was keeping concentrations at 8×10^7 sperm/ml or less. Higher concentrations resulted in a greater proportion of intact sperm and fewer tails broken into fragments. Analysis of electron micrographs indicated that the longest fibrous sheath fragments were the ones that contained contaminating filamentous material in the lumen, suggesting that the extraction of other cytoskeletal elements was most efficient on shorter flagellar fragments. Following the sonication step, nuclei were eliminated by low-speed centrifugation, with multiple resuspensions of the pellet to improve recovery of the tail fragments.

A key aspect of the extraction protocol developed in this study was the length and force of the centrifugation following the final extraction with urea. Alterations of other factors, including extraction time, pH, and the concentration of DTT, KSCN, or urea, did not result in substantial reductions in contaminating cytoskeletal proteins. However, fibrous sheath purities were markedly improved when the final centrifugation step was optimized at $32\,500 \times g$ for 12 min. The use of greater force and/or longer time resulted in preparations with significant axonemal and outer dense fiber contamination.

Fibrous sheaths isolated in previous studies often retained some filamentous material within the lumen [32–34, 41], suggested to be remnants of outer dense fibers or central extensions of the fibrous sheath [32]. In addition to ultrastructural analysis, we used antibodies specific for proteins of the fibrous sheath (AKAP4), the axoneme (α-tubulin), and the outer dense fibers (ODF2) to assess the enrichment and purity of our fibrous sheath fraction. Western blotting data indicated that the quantity of AKAP4 increased throughout the protocol, while α-tubulin and ODF2 were reduced to ~5% and ~2% of original levels, respectively. These data demonstrate that the procedure used in this study was very efficient in eliminating contaminating cytoskeletal components from the final fibrous sheath fraction and strengthen the conclusion that multiple glycolytic enzymes are tightly bound to this cytoskeletal structure.

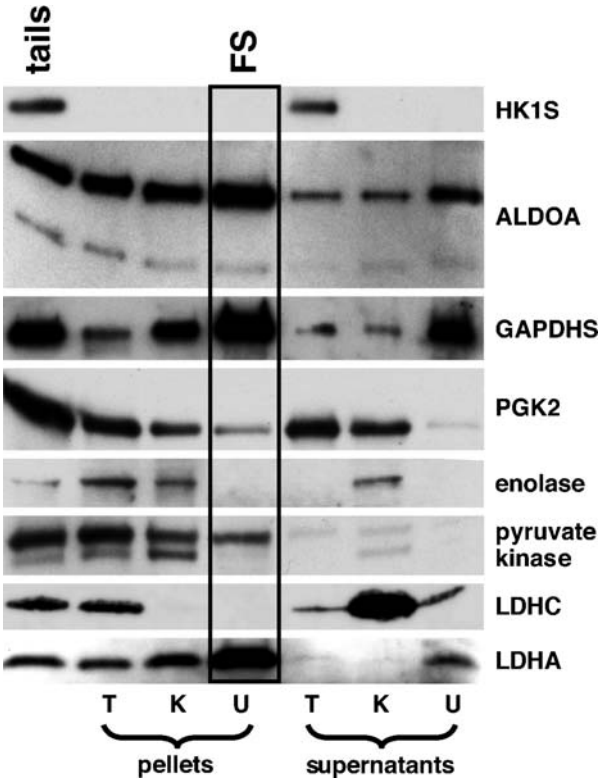

FIG. 7. Western blot analyses examining the extraction of multiple glycolytic enzymes during the fibrous sheath isolation procedure. Specific antibodies used for each blot are indicated on the right. All glycolytic enzymes examined were present in flagella isolated from 10^6 sperm (lane 1, tails). The tail fraction was sequentially extracted with buffers containing 1% Triton X-100 (T), 0.6 M KSCN (K), and 6 M urea (U), and aliquots were removed from each pellet and supernatant for Western analysis. Equal protein amounts were loaded in each lane. ALDOA, GAPDHS, pyruvate kinase, LDHA, and a small amount of PGK2 were detected in isolated fibrous sheaths (FS) remaining in the urea pellet.

The final fibrous sheath pellet was resolved into 18 protein bands following one-dimensional SDS-PAGE and SYPRO Ruby staining. Densitometric analyses indicated that the fibrous sheath fraction contained approximately 10% of the amount of protein present in the starting material. AKAP4, AKAP3, GAPDHS, and GSTM5, four known fibrous sheath constituents [reviewed in 17], were identified in this fraction by MS. As expected, AKAP4 was the most prominent fibrous sheath protein. In addition to the major 82 000 molecular weight form, proteomic analysis identified several minor bands as AKAP4. The four bands with molecular weights >220 000 may be aggregates of AKAP4 proteins. Pro-AKAP4 is a 109 000 molecular weight protein that is processed to 82 000 and 26 000 molecular weight proteins when AKAP4 is assembled into the fibrous sheath [49]. We detected multiple forms smaller than 82 000 but greater than 26 000. It is unclear whether these bands resulted from limited proteolysis during the fibrous sheath isolation or may correspond to aggregates containing the 26 000 molecular weight fragment. Although several glycolytic enzymes are localized in the principal piece of mammalian sperm, only GAPDHS was previously shown to be tightly bound to the fibrous sheath [4, 5]. This study determined that two additional glycolytic enzyme subunits, ALDOA and LDHA, are prominent constituents of the fibrous sheath.

In the glycolytic pathway, aldolase catalyzes the cleavage of fructose-1,6-bisphosphate to glyceraldehyde-3-phosphate and dihydroxyacetone phosphate. One of three aldolase subunits, ALDOA is expressed in most tissues, with high concentrations in skeletal muscle [60]. Expression of the other subunits is more restricted, with ALDOB prominent in liver and ALDOC in brain and neuronal tissue [60, 61]. Two fibrous sheath proteins with apparent molecular weights of 50 000 and 41 000 were identified as ALDOA by peptide-mass fingerprinting and MS/MS peptide fragment ion matching. The smaller band migrates close to the calculated molecular weight of 39 331 for ALDOA. However, the 50 000 molecular weight band migrates at a size approximately 25% greater than expected. This is similar to the situation with the GAPDHS subunit, which has a predicted molecular weight of 47 455 yet migrates at ~69 000 on SDS gels because of a proline-rich N-terminal segment [5]. The aberrant migration of the larger ALDOA band may indicate posttranslational modifications or a novel protein sequence in spermatogenic cells. Although a unique aldolase protein has not been reported in mammalian spermatogenic cells or sperm, bovine sperm aldolase has distinctive kinetic properties [28]. Analyses are under way to determine whether sperm contain ALDOA or a novel isozyme that shares a common sequence with ALDOA.

Multiple LDH isozymes catalyze the interconversion of pyruvate and lactate and use NAD^+ as a coenzyme. Expression of the LDH C subunit is restricted to spermatogenic cells and oocytes, and the LDHC homotetramer (LDH-C_4) is the only LDH isozyme previously detected in mouse sperm [62–64]. This sperm-specific isozyme has distinctive catalytic properties, including insensitivity to lactate inhibition [64], which may be essential for maintaining the high glycolytic activity that supports sperm motility [10]. Although LDHC is localized predominantly in the principal piece [8], ~50% of this isozyme was released during sonication, and the remainder was not retained in the fibrous sheath fraction in our studies. Both proteomic and Western analyses identified LDHA but not LDHC in fibrous sheaths isolated from mouse sperm. The homotetramer of the LDHA (LDH-A_4 or LDH-5) is the predominant isozyme in skeletal muscle, with kinetic properties that facilitate the rapid reduction of pyruvate to lactate under anaerobic conditions [65]. LDH isozymes containing the LDHA subunit are present throughout spermatogenesis, although they are not as prominent as LDH isozymes containing the LDHB subunit [63]. A novel *Ldha* mRNA with a distinct first exon has been identified in both mouse [66] and human [67] testis, and the protein was detected in a lipid raft fraction isolated from mouse sperm [68]. Further studies are needed to determine the expression profile of this novel transcript and the characteristics of the protein that it encodes.

Western analysis of sperm tail fractions taken at each step throughout the fibrous sheath isolation procedure allowed us to determine the relative solubilities of seven glycolytic enzymes in the sperm flagellum. Spermatogenic cell-specific HK1S variants detected with the SSR peptide-specific antibody were found only in the Triton X-100 supernatant, consistent with a previous report that sperm hexokinase activity is completely solubilized with this detergent [9]. Similarly, enolase was solubilized with the KSCN extraction buffer and was not detected in the fibrous sheath. Low levels of PGK2 were detected in some fibrous sheath preparations, although the amount was significantly reduced compared to the initial sperm tail fraction. Significant fractions of both enolase and PGK2 were released by the initial sonication step used in our isolation procedure.

Four glycolytic enzymes, ALDOA, GAPDHS, LDHA, and pyruvate kinase, were consistently detected in the fibrous sheath by Western blotting. The first three of these enzymes were also identified as fibrous sheath constituents by peptide-mass fingerprinting or MS/MS peptide fragment ion matching. These proteomic approaches did not detect pyruvate kinase, perhaps because it migrates on SDS gels near GAPDHS. It is likely that the pyruvate kinase present in sperm is the skeletal muscle isozyme (M1 encoded by the *Pkm2* gene) since expression of this form increases in the testis with the appearance of elongating spermatids [69]. In addition, we used an antibody raised against rabbit muscle pyruvate kinase, although it has not been determined if this antibody cross-reacts with other pyruvate kinase isozymes. Fibrous sheaths isolated from GAPDHS knockout mice [10] may be useful for further identification of the pyruvate kinase isozyme present in this cytoskeletal structure.

In conclusion, the protocol developed in this study generated a fibrous sheath fraction approximately 95% free of axonemal and outer dense fiber contamination. Proteomic and Western analyses identified the major protein constituents of the mouse fibrous sheath following separation by one-dimensional SDS-PAGE, including four glycolytic enzymes. Although only a subset of glycolytic enzymes was examined by Western blotting, the results support the hypothesis that the fibrous sheath plays an important role in regulating ATP production required for sperm motility. Additional studies to examine the association of the remaining glycolytic enzymes with the fibrous sheath would clearly provide valuable information.

ACKNOWLEDGMENTS

We thank Ms. Victoria Madden for preparing samples for transmission electron microscopy; Dr. C. Robert Bagnell for the use of the transmission electron microscope; Dr. Carol Parker at the UNC Proteomics Core Facility for mass spectrometry analyses; Dr. E.M. Eddy for antibodies to AKAP4, HK1S, and GAPDHS; Dr. Frans A. van der Hoorn for the ODF2 antibody; Drs. John McCarrey and John VandeBerg for the PGK2 antibody; and Dr. Erwin Goldberg for the LDHC antibody.

REFERENCES

1. Kamp G, Busselmann G, Lauterwein J. Spermatozoa: models for studying regulatory aspects of energy metabolism. Experientia 1996; 52:487–494.
2. Mori C, Nakamura N, Welch J, Gotoh H, Goulding E, Fujioka M, Eddy M. Mouse spermatogenic cell-specific type 1 hexokinase (*mHK1-s*) transcripts are expressed by alternative splicing from the *mHk1* gene and the HK1-S protein is localized mainly in the sperm tail. Mol Reprod Dev 1998; 49:374–385.
3. Travis AJ, Foster JA, Rosenbaum NA, Visconti PE, Gerton GL, Moss SB. Targeting of a germ cell-specific hexokinase lacking a porin-binding domain to the mitochondria as well as to the head and fibrous sheath of murine spermatozoa. Mol Biol Cell 1998; 9:263–276.
4. Westhoff D, Kamp G. Glyceraldehyde 3-phosphate dehydrogenase is bound to the fibrous sheath of mammalian spermatozoa. J Cell Sci 1997; 110:1821–1829.
5. Bunch DA, Welch JE, Magyar PL, Eddy EM, O'Brien DA. Glyceraldehyde 3-phosphate dehydrogenase-S protein distribution during mouse spermatogenesis. Biol Reprod 1998; 58:834–841.
6. Welch JE, Brown PL, O'Brien DA, Magyar PL, Bunch DO, Mori C, Eddy EM. Human glyceraldehyde 3-phosphate dehydrogenase-2 gene is expressed specifically in spermatogenic cells. J Androl 2000; 21:328–338.
7. Gitlits VM, Toh BH, Loveland KL, Sentry JW. The glycolytic enzyme enolase is present in sperm tail and displays nucleotide-dependent association with microtubules. Eur J Cell Biol 2000; 79:104–111.
8. Beyler SA, Wheat TE, Goldberg E. Binding of antibodies against antigenic domains of murine lactate dehydrogenase-C_4 to human and mouse spermatozoa. Biol Reprod 1985; 2:1201–1210.
9. Travis AJ, Jorgez CJ, Merdiushev T, Jones BH, Dess DM, Diaz-Cueto L, Storey BT, Kopf GS, Moss SB. Functional relationships between

capacitation-dependent cell signaling and compartmentalized metabolic pathways in murine spermatozoa. J Biol Chem 2001; 276:7630–7636.
10. Miki K, Qu W, Goulding EH, Willis WD, Bunch DO, Strader LF, Perreault SD, Eddy EM, O'Brien DA. Glyceraldehyde 3-phosphate dehydrogenase-S, a sperm-specific glycolytic enzyme, is required for sperm motility and male fertility. Proc Natl Acad Sci U S A 2004; 101: 16501–16506.
11. Mukai C, Okuno M. Glycolysis plays a major role for adenosine triphosphate supplementation in mouse sperm flagellar movement. Biol Reprod 2004; 71:540–547.
12. Wojtas K, Slepecky N, von Kalm L, Sullivan D. Flight muscle function in Drosophila requires colocalization of glycolytic enzymes. Mol Biol Cell 1997; 8:1665–1675.
13. Sullivan DT, MacIntyre R, Fuda N, Fiori J, Barrilla J, Ramizel L. Analysis of glycolytic enzyme co-localization in Drosophila flight muscle. J Exp Biol 2003; 206:2031–2038.
14. Fawcett DW. The mammalian spermatozoon. Dev Biol 1975; 44:394–436.
15. Storey BT, Kayne FJ. Energy metabolism of spermatozoa. V. The Embden-Myerhof pathway of glycolysis: activities of pathway enzymes in hypotonically treated rabbit epididymal spermatozoa. Fertil Steril 1975; 26:1257–1265.
16. Brooks DE. Activity and androgenic control of glycolytic enzymes in the epididymis and epididymal spermatozoa of the rat. Biochem J 1976; 156: 527–537.
17. Eddy EM, Toshimori K, O'Brien DA. Fibrous sheath of mammalian spermatozoa. Microsc Res Tech 2003; 61:103–115.
18. Turner RM. Tales from the tail: what do we really know about sperm motility? J Androl 2003; 24:790–803.
19. Fenderson BA, Toshimori K, Muller CH, Lane TF, Eddy EM. Identification of a protein in the fibrous sheath of the sperm flagellum. Biol Reprod 1988; 38:345–357.
20. Eddy EM, Welch JE, Mori C, Fulcher KD, O'Brien DA. Role and regulation of spermatogenic cell-specific gene expression: enzymes of glycolysis. In: Bartke A, (ed.), Function of Somatic Cells in the Testis. New York: Springer-Verlag; 1994:362–372.
21. Welch JE, Schatte EC, O'Brien DA, Eddy EM. Expression of a glyceraldehyde 3-phosphate dehydrogenase gene specific to mouse spermatogenic cells. Biol Reprod 1992; 46:869–878.
22. Edwards YH, Povey S, LeVan KM, Driscoll CE, Millan JL, Goldberg E. Locus determining the human sperm-specific lactate dehydrogenase, LDHC, is syntenic with LDHA. Dev Genet 1987; 8:219–232.
23. Sakai I, Sharief FS, Li SSL. Molecular cloning and nucleotide sequence of the cDNA for sperm-specific lactate dehydrogenase-C from mouse. Biochem J 1987; 242:619–622.
24. McCarrey JR, Thomas K. Human testis-specific PGK gene lacks introns and possesses characteristics of a processed gene. Nature 1987; 326:501–505.
25. Boer PH, Adra CN, Lau YF, McBurney MW. The testis-specific phosphoglycerate kinase gene *Pgk-2* is a recruited retroposon. Mol Cell Biol 1987; 7:3107–3112.
26. Mori C, Welch JE, Fulcher KD, O'Brien DA, Eddy EM. Unique hexokinase messenger ribonucleic acids lacking the porin-binding domain are developmentally expressed in mouse spermatogenic cells. Biol Reprod 1993; 49:191–203.
27. Buehr M, McLaren A. An electrophoretically detectable modification of glucosephosphate isomerase in mouse spermatozoa. J Reprod Fertil 1981; 63:169–173.
28. Gillis BA, Tamblyn TM. Association of bovine sperm aldolase with sperm subcellular components. Biol Reprod 1984; 31:25–35.
29. Russell DL, Kim KH. Expression of triosephosphate isomerase transcripts in rat testis: evidence for retinol regulation and a novel germ cell transcript. Biol Reprod 1996; 55:11–18.
30. Fundele R, Winking H, Illmensee K, Jagerbauer E-M. Developmental activation of phosphoglycerate mutase-2 in the testis of the mouse. Dev Biol 1987; 124:562–566.
31. Edwards YH, Grootegoed JA. A sperm-specific enolase. J Reprod Fertil 1983; 68:305–310.
32. Olson GE, Hamilton DW, Fawcett DW. Isolation and characterization of the fibrous sheath of rat epididymal spermatozoa. Biol Reprod 1976; 14: 517–530.
33. Oko R. Comparative analysis of proteins from the fibrous sheath and outer dense fibers of rat spermatozoa. Biol Reprod 1988; 39:169–182.
34. Brito M, Figueroa J, Maldonado EU, Vera JC, Burzio LO. The major component of the rat sperm fibrous sheath is a phosphoprotein. Gamete Res 1989; 22:205–217.
35. Kim YH, McFarlane JR, Almahbobi G, Stanton PG, Temple-Smith PD, de Krester DM. Isolation and partial characterization of rat sperm tail fibrous sheath proteins and comparison with rabbit and human spermatozoa using a polyclonal antiserum. J Reprod Fertil 1995; 104:107–114.
36. Brito M, Burzio LO. Isolation of the fibrous sheath of mammalian sperm flagella. Methods Cell Biol 1995; 47:391–395.
37. Eddy EM, O'Brien DA, Fenderson BA, Welch JE. Intermediate filament-like proteins in the fibrous sheath of the mouse sperm flagellum. Ann N Y Acad Sci 1991; 637:224–239.
38. Fujinoki M, Kawamura T, Toda T, Ohtake H, Ishimoda-Takagi T, Shimizu N, Yamaoka S, Okuno M. Identification of 36 kDa phosphoprotein in fibrous sheath of hamster spermatozoa. Comp Biochem Physiol B Biochem Mol Biol 2004; 137:509–520.
39. Kim YH, de Krester DM, Temple-Smith PD, Hearn MTW, McFarlane JR. Isolation and characterization of human and rabbit sperm tail fibrous sheath. Mol Hum Reprod 1997; 3:307–313.
40. Jassim A, Gillot DJ, Al-Zuhdi Y, Gray A, Foxton R, Bottazzo GF. Isolation and biochemical characterization of the human sperm tail fibrous sheath. Hum Reprod 1992; 7:86–94.
41. Ricci M, Breed WG. Isolation and partial characterization of the outer dense fibres and fibrous sheath from the sperm tail of a marsupial: the brushtail possum (*Trichosurus vulpecula*). Reproduction 2001; 121:373–388.
42. Miki K, Willis WD, Brown PR, Goulding EH, Fulcher KD, Eddy EM. Targeted disruption of the AKAP4 gene causes defects in sperm flagellum and motility. Dev Biol 2002; 248:331–342.
43. Shao X, Tarnasky HA, Schalles U, Oko R, van der Hoorn FA. Interactional cloning of the 84-kDa major outer dense fiber protein Odf84. Leucine zippers mediate associations of Odf84 and Odf27. J Biol Chem 1997; 272:6105–6113.
44. Hintz M, Goldberg E. Immunohistochemical localization of LDH-X during spermatogenesis in mouse testes. Dev Biol 1977; 57:375–384.
45. Borchers C, Peter JF, Hall MC, Kunkel TA, Tomer KB. Identification of in-gel digested proteins by complementary peptide-mass fingerprinting and tandem mass spectrometry data obtained on an electrospray ionization quadrupole time-of-flight mass spectrometer. Anal Chem 2000; 72:1163–1168.
46. Parker CE, Warren MR, Loiselle DR, Dicheva NN, Scarlett CO, Borchers CH. Identification of components in protein complexes. Methods Mol Biol 2005; 301:117–151.
47. Carrera A, Gerton GL, Moss SB. The major fibrous sheath polypeptide of mouse sperm: structural and functional similarities to the A-kinase anchoring proteins. Dev Biol 1994; 165:272–284.
48. Fulcher KD, Mori C, Welch JE, O'Brien DA, Klapper DG, Eddy EM. Characterization of *Fsc1* cDNA for a mouse sperm fibrous sheath component. Biol Reprod 1995; 52:41–49.
49. Johnson LR, Foster JA, Haig-Ladewig L, VanScoy H, Rubin C, Moss SB, Gerton GB. Assembly of AKAP82, a protein kinase A anchor protein, into the fibrous sheath of mouse sperm. Dev Biol 1997; 192:340–350.
50. Visconti PE, Johnson LR, Oyaski M, Fornes M, Moss SB, Gerton GL, Kopf GS. Regulation, localization, and anchoring of protein kinase A subunits during mouse sperm capacitation. Dev Biol 1997; 192:351–363.
51. Miki K, Eddy EM. Identification of tethering domains for protein kinase A type Iα regulatory subunits on sperm fibrous sheath protein FSC1. J Biol Chem 1998; 273:34384–34390.
52. Brown P, Miki K, Harper DB, Eddy EM. A-kinase anchoring protein 4 binding proteins in the fibrous sheath of the sperm flagellum. Biol Reprod 2003; 68:2241–2248.
53. Mandal A, Naaby-Hansen S, Wolkowicz MJ, Klotz K, Shetty J, Retief JD, Coonrod SA, Kinter M, Sherman N, Cesar F, Flickinger CJ, Herr JC. FSP95, a testis-specific 95-kilodalton fibrous sheath antigen that undergoes tyrosine phosphorylation in capacitated human spermatozoa. Biol Reprod 1999; 61:1184–1197.
54. Fulcher KD, Welch JE, Klapper DG, O'Brien DA, Eddy EM. Identification of a unique μ-class glutathione S-transferase in mouse spermatogenic cells. Mol Reprod Dev 1995; 42:415–424.
55. Hoshi K, Tsukikawa S, Sato A. Importance of Ca 2+, K+, and glucose in the medium for sperm penetration through the human zona pellucida. Tohoku J Exp Med 1991; 165:99–104.
56. Williams AC, Ford WC. The role of glucose in supporting motility and capacitation in human spermatozoa. J Androl 2001; 22:680–695.
57. Srere PA, Knull HR. Location-location-location. Trends Biochem Sci 1998; 23:319–320.
58. Ikemoto A, Bole DG, Ueda T. Glycolysis and glutamate accumulation into synaptic vesicles. Role of glyceraldehyde phosphate dehydrogenase and 3-phosphoglycerate kinase. J Biol Chem 2003; 278:5929–5940.
59. Wu K, Aoki C, Elste A, Rogalski-Wilk AA, Siekevitz P. The synthesis of ATP by glycolytic enzymes in the postsynaptic density and the effect of

endogenously generated nitric oxide. Proc Natl Acad Sci U S A 1997; 94: 13273–13278.
60. Penhoet E, Rajkumar T, Rutter WJ. Multiple forms of fructose diphosphate aldolase in mammalian tissues. Proc Natl Acad Sci U S A 1966; 56:1275–1282.
61. Penhoet EE, Kochman M, Rutter WJ. Molecular and catalytic properties of aldolase C. Biochemistry 1969; 8:4396–4402.
62. Coonrod S, Vitale A, Duan C, Bristol-Gould S, Herr J, Goldberg E. Testis-specific lactate dehydrogenase (LDH-C4; Ldh3) in murine oocytes and preimplantation embryos. J Androl 2006; Apr 1, Epub ahead of print as doi:10.2164/jandrol.05185.
63. Li SSL, O'Brien DA, Hou EW, Versola J, Rockett DL, Eddy EM. Differential activity and synthesis of lactate dehydrogenase isozymes A (muscle), B (heart), and C (testis) in mouse spermatogenic cells. Biol Reprod 1989; 40:173–180.
64. Goldberg E. Isozymes in testes and spermatozoa. Isozymes Curr Top Biol Med Res 1977; 1:79–124.
65. Markert CL. Lactate dehydrogenase: biochemistry and function of lactate dehydrogenase. Cell Biochem Funct 1984; 2:131–134.
66. Hiraoka BY, Li SSL. Lactate dehydrogenase-A mRNA in mouse testis and somatic tissues contain different 5′ noncoding sequences. J Genet Mol Biol 1990; 1:1–6.
67. Maekawa M, Inomata M, Sasaki MS, Kaneko A, Ushiama M, Sugano K, Takayama J, Kanno T. Electrophoretic variant of a lactate dehydrogenase isoenzyme and selective promoter methylation of the LDHA gene in a human retinoblastoma cell line. Clin Chem 2002; 48:1938–1945.
68. Sleight SB, Miranda PV, Plaskett NW, Maier B, Lysiak J, Scrable H, Herr JC, Visconti PE. Isolation and proteomic analysis of mouse sperm detergent-resistant membrane fractions: evidence for dissociation of lipid rafts during capacitation. Biol Reprod 2005; 73:721–729.
69. de Luis O, del Mazo J. Gene expression of mouse M1 and M2 pyruvate kinase isoenzymes correlates with differential poly[A] tract extension of their mRNAs during the development of spermatogenesis. Biochim Biophys Acta 1998; 1396:294–305.